A singular perturbation approach for the control of electromagnetic actuators

Yassine Ariba, Frédéric Gouaisbaut

A singular perturbation approach for the control of electromagnetic actuators

Yassine Ariba * **Frédéric Gouaisbaut** *

* *LAAS-CNRS, Université de Toulouse, INSA, UPS, Toulouse, France (e-mail: yariba@laas.fr, fgouaisb@laas.fr).*

Abstract: The paper is devoted to the control of electromagnetic actuators. Compared to most results in the literature, the design explicitly takes into account the nonlinearities and the magnetic saturation. An approach based on singularly perturbed systems is proposed to take advantage of the different time scales of the model and provide a minimal complexity control law. Associated with an integral action, this control law ensures accuracy and robustness w.r.t some disturbances and some unknown parameters of the actuator. The use of the singular perturbation method allows also to limit the implementation complexity compared to classical methods such as backstepping control. The synthesis of the control law is then tested through simulations that illustrate the efficiency of the method.

Keywords: Electromagnetic actuator, nonlinear control application, Lyapunov method, singular perturbation method

1. INTRODUCTION

In recent years, many industrial technologies have witnessed the increasing use of electromagnetic actuators (EMA) due to their high precision compared to more classical actuators, Chen et al. (2004). Such devices can be found at the heart of systems as micropositioning Cugat et al. (2003), suspension or levitation control for railway vehicles Foo and Goodall (2000); Lee et al. (2006) or hydraulic valves in cars or space industries Deschaux et al. (2019), paper or plate production Jin et al. (1998) to cite a few applications.

Even if the technology has matured, the precision of such a device comes at the price of a more consequent effort to control them (see Boldea (2003); Forrai (2018) and references therein) and it therefore raises many theoretical issues. Indeed, the dynamics driving an electromagnetic actuator are highly nonlinear which makes the control design complicated. If one aims at designing a highly precise and fast actuators, it is often necessary to take into account the phenomena of magnetic saturation and flux fringing. The first phenomenon is related to the saturation of the magnetic flux and leads to the saturation of the magnetic force limiting the capacities of the actuator Deschaux et al. (2018, 2019). The second well-known phenomenon is related to the flux leakage in the air gap Zhang et al. (2022). This effect is generally difficult to model and results in a partial misunderstanding of the inductance of the magnetic circuit Deschaux (2020).

In the literature, numerous works are based on linear models (usually constructed from a linearization around an operating point) to design some classical proportional, proportional integral control laws Forrai (2018), state feedback based on geometric approach Mercorelli (2017) or Model Predictive Control, Di Cairano et al. (2007). Notice that these approaches have been extended in a Linear Parameter Varying framework in Forrai et al. (2007). Obviously, these approaches are effective locally, i.e. close to the operating point. For broader use, many researches have turned to nonlinear controls to deal with more relevant models, as for instance Control Lyapunov Function, Peterson et al. (2006), Flatness based control, Robert Koch et al. (2002),Mercorelli et al. (2003), Sliding Mode Control Mercorelli (2012)), Nguyen et al. (2007) to see a few. Among the many methods considered, backstepping methods are the most common tools to design efficient control laws based on a nonlinear model of the actuators Kahveci and Kolmanovsky (2010), Schwarzgruber et al. (2012) and references therein. Indeed, given the cascade structure of the system, i.e. an electromagnetic subsystem controlling a mechanical structure, many backstepping designs have been proposed to ensure the closed loop stability of the overall system. Nevertheless, few them have taken into account all the nonlinearities like the magnetic saturation, Deschaux et al. (2019).

In this paper, we propose to design a control law based on a nonlinear model, taking into account not only the nonlinearities resulting from the calculation of the magnetic flux, but also the variation of the inductance w.r.t. the position of the mechanical body and more particularly the magnetic saturation. Moreover, in order to consider the different dynamics of the physical systems involved (electrical, magnetic and mechanical subsystems), we turned to a synthesis of control laws based on singularly perturbed systems, Kokotović et al. (1999). The key idea is to separate the design process into two steps so as to eventually obtain a simplified control law while ensuring the asymptotic stability of the overall closed-loop system. The slow system consists of the mechanical subsystem whose driving force law has been virtually chosen to ensure a trajectory tracking with some performance requirements. The fast system corresponds to the electrical subsystem

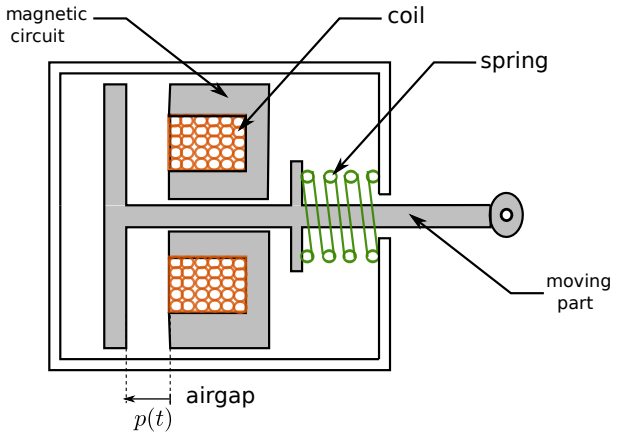

Fig. 1. *Scheme of the actuator.*

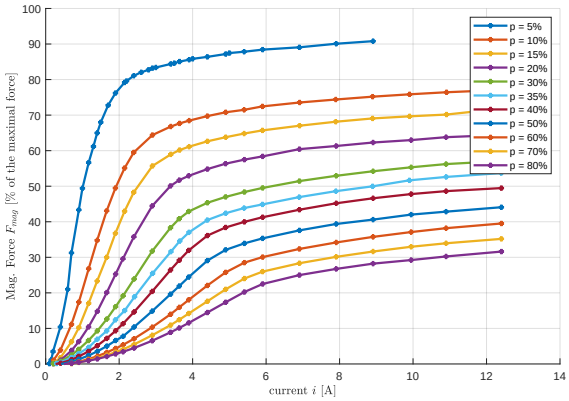

Fig. 2. *Experimental characterization of F_{mag} with respect to the current i and the airgap p (as a percentage of the maximal displacement).*

for which we design the voltage control law to make the actual current converges to the ideal one required to induce the desired magnetic force for the mechanical slow subsystem. Furthermore, in order to obtain a precise closed-loop system, an integral action is also added to the nonlinear design. This feature allows to compensate for disturbance force (or uncertain force/parameters) affecting the mechanical positioner.

The paper is organized as follows. Section 2 deals with the description of the system and its modeling as a singularly perturbed system. Section 3 is devoted to the control design. Section 4 shows some simulation results to illustrate the proposed methodology. Lastly, a conclusion is given in Section 5.

2. DESCRIPTION OF THE SYSTEM

2.1 Physical system

The studied actuator is depicted in Figure 1. The mechanism is made of a coil winding a magnetic circuit, itself composed of a fixed frame and a moving part. The distance between these two parts is the airgap and it influences the magnetic flux. The control variable is the voltage at the coil terminals, and the resulting current induces a magnetic force which tends to close the airgap (unidirectional force, toward right). The spring is used to counteract the magnetic force and pushes the moving part to the left.

2.2 Modeling

Physical modeling
The model can be divided in three distinct parts : mechanical, electrical and magnetic parts. Regarding the first one, the mechanical subsystem is a simple mass-spring system that can be modeled with the Newton's second law :

$$m\frac{d^2p(t)}{dt^2} = -F_{mag} - \lambda\frac{dp(t)}{dt} - K\big(p(t) - l_0\big), \qquad (1)$$

where F_{mag} is the magnetic force induced by the coil current, the second and third terms in the right-hand side represent respectively the friction and the spring forces. Parameters λ and K are the friction and stiffness coefficients, l_0 is the natural length of the spring and m is the mass of the moving part.

The electrical part stems from the coil controlled by the voltage u:

$$u(t) = Ri(t) + L(p)\frac{di(t)}{dt} + i\frac{dL(p)}{dt},$$

with i the current flowing through the coil and R its electrical resistance. The third term in the right-hand side is due to the fact that the inductance of the system L is varying and depends on the airgap $p(t)$ via the magnetic circuit. Hence, the electrical equation becomes

$$u(t) = Ri(t) + L\frac{di(t)}{dt} + i\frac{\partial L}{\partial p}\frac{dp(t)}{dt} \qquad (2)$$

The magnetic phenomena, induced by current i flowing through the coil, generate the driving force F_{mag} that allows to move the mechanical part. This force actually depends both on the current and the airgap, its modeling is therefore a crucial step in the control of EMA. Various models exist in the literature and consider different hypothesis, leading to more or less accurate representation of the process, to develop suitable design methods. Only few of them (Zhang et al. (2022) and references therein) take into account the magnetic saturation of the magnetic circuit which is specific to the material. This phenomenon has a substantial impact on the value of the force and cannot be neglected. Then, an experimental characterization have been set up to identify a function $F_{mag}(p, i)$ w.r.t. the airgap and the current, Deschaux et al. (2019). Results of the experiment are plotted in Figure 2. Regarding the circuit inductance, L which depends on the airgap has been identified via a finite element method software. In the sequel, we will consider that L is a small quantity ($L(p) < 0.09\,H$ in our case).

Gathering equations (1) and (2) and defining the position p and velocity v of the moving part, and the current i as state variables, a state space modeling for the EMA is obtained :

$$\begin{cases} \dfrac{dp}{dt} = v \\ \dfrac{dv}{dt} = \dfrac{1}{m}\Big(- F_{mag}(p,i) - \lambda v - K\Big(p - l_0\Big) + F_d \Big) \\ \dfrac{di}{dt} = \dfrac{1}{L}\Big(u - Ri - iv\dfrac{\partial L}{\partial p}\Big) \end{cases} \qquad (3)$$

Furthermore, one considers an additional force F_d which represents an unknown constant (or slowly time varying) force that disturbs the mechanical system. This disturbance may also encompasses uncertainty on the natural spring length l_0.

The purpose of the paper is:

- To model electromagnetic actuators as a singularly perturbed system highlighting the different dynamics involved.
- To determine a control law based on the previous model allowing to stabilize the position of the mechanical part at a given operating point with some accuracy and robustness properties.
- To benefit from the decoupling of the dynamics to derive a minimal complexity control law for the sake of implementation simplification and reliability.

At this stage, it is important to understand that this system is a multi-physical system which naturally admits very different response times. The electrical part is indeed much faster than the mechanical part. Considering these physical features, we have focused our control techniques on singular perturbations method popularized by Kokotović et al. (1999).

Singular perturbation system modeling
In order to control the position of the actuator, that is to make p converges to a given constant reference r, we aim at reworking the above model. As a first step, in order to cope with the static error, let consider the mechanical subsystem (the two first equations of (3)) and let us introduce an integral action with a new state variable η. Regarding the well-known integral action, it is a useful control technique to eliminate the steady state error.

$$\begin{cases} \dfrac{d\eta}{dt} = p - r \\ \dfrac{dp}{dt} = v \\ \dfrac{dv}{dt} = \dfrac{1}{m}\Big(- F_{mag} - \lambda v - K\Big(p - l_0\Big) + F_d \Big) \end{cases} \tag{4}$$

As in a backstepping approach, Khalil (2002), let us consider the magnetic force as a virtual control input force F_u, which is designed as a state feedback law to control the above linear mechanical system:

$$F_u = \gamma_0\, \eta + \gamma_1\, p + \gamma_2\, v = \Gamma \begin{bmatrix} \eta \\ p \\ v \end{bmatrix} = \Gamma \xi \tag{5}$$

with $\gamma_0 \in \mathbb{R}^*$, $\gamma_1 \in \mathbb{R}$ and $\gamma_2 \in \mathbb{R}$ scalar gains to be tuned. ξ denotes the state of (4). Combining the subsystem (4) and the virtual control (5), one obtained the virtual closed loop system:

$$\begin{cases} \dfrac{d\eta}{dt} = p - r \\ \dfrac{dp}{dt} = v \\ \dfrac{dv}{dt} = \dfrac{1}{m}\Big(- \gamma_0\eta - (\gamma_1 + K)p - (\gamma_2 + \lambda)v + Kl_0 + F_d \Big) \end{cases}$$

which possesses a unique equilibrium point

$$\begin{cases} \eta^\star = \dfrac{1}{\gamma_0}\Big(K(l_0 - r) - \gamma_1 r + F_d\Big) \\ p^\star = r \\ v^\star = 0 \end{cases}$$

Defining now the deviation vector x w.r.t. the equilibrium point

$$x = \begin{bmatrix} x_0 \\ x_1 \\ x_2 \end{bmatrix} = \begin{bmatrix} \eta - \eta^\star \\ p - p^\star \\ v - v^\star \end{bmatrix} = \xi - \xi^*$$

the following new virtual closed-loop dynamical system is to be studied

$$\dot{x} = \begin{bmatrix} 0 & 1 & 0 \\ 0 & 0 & 1 \\ -\dfrac{\gamma_0}{m} & -\dfrac{\gamma_1 + K}{m} & -\dfrac{\gamma_2 + \lambda}{m} \end{bmatrix} x \tag{6}$$

Control gain Γ of (5) can then be easily designed to stabilize the mechanical system with some required performances and robustly w.r.t. parameters K and λ. Remark that the term $\eta^\star$, likely unknown, is not used in the control law (5) and will be actually compensated by the integral control action.

We now need to take into account the deviation between the desired force F_u for our control objective and the actual magnetic force F_{mag} induced by the electrical part. Theory and experimentation (see Figure 2) show that F_{mag} is strictly monotonic both w.r.t. the position and the current. Hence, for a given desired F_u and a position p, a unique corresponding desired current i_d can be computed. Note that i_d is a function of the entire extended mechanical states x. Let us denote the difference between the desired current and the actual one $z = i - i_d$. With these notations, the original mechanical subsystem (4) is equivalently rewritten as

$$\dot{x} = \underbrace{\begin{bmatrix} 0 & 1 & 0 \\ 0 & 0 & 1 \\ -\dfrac{\gamma_0}{m} & -\dfrac{\gamma_1 + K}{m} & -\dfrac{\gamma_2 + \lambda}{m} \end{bmatrix}}_{A} x + \underbrace{\begin{bmatrix} 0 \\ 0 \\ \dfrac{1}{m} \end{bmatrix}}_{B} \delta(x, z) \tag{7}$$

with $\delta(x, z) = F_u - F_{mag}(p, i) = F_u - F_{mag}(x_1 + r, z + i_d)$ corresponds to the error between the desired force and the actual one. Note that we have $F_u = F_{mag}(x_1 + r, i_d)$. The desired current $i_d(x) = F_{mag}^{-1}(F_u, x_1 + r)$ for the ideal control law F_u is a static function of $[\eta, p, v]^T$, and can be straightforwardly expressed as a function of x. F_{mag}^{-1} stands for the reciprocal function of F_{mag} for a chosen $p = x_1 + r$.

The second step of our modeling is to assess the derivative of z, and thus to make the link with the electrical part:

$$\begin{aligned} \dot{z} &= \frac{1}{L}\left(u - Ri - iv\frac{\partial L}{\partial p}\right) - \frac{di_d}{dt} \\ &= \frac{1}{L}\left(u - \left(R + x_2\frac{\partial L}{\partial x_1}\right)\Big(z + i_d\Big)\right) - \frac{di_d}{dt} \end{aligned}$$

The second line expresses the dynamic of z in the (x, z) state variables. Note that the desired current is a known nonlinear static function of x. Based on the fact that the inductance L is a small quantity and that the current dynamic is much faster than the mechanical dynamic, we aim at exploiting this feature and model the system in the framework of singular perturbation system Khalil (2002); Kokotović et al. (1999). Denoting $\varepsilon = L$, the whole system can be rewritten as

$$\begin{aligned} \dot{x} &= f(x,z) \\ \varepsilon\dot{z} &= g(x,z,\varepsilon) \end{aligned} \tag{8}$$

with

$$f(x,z) = Ax + B\delta(x,z)$$

$$g(x,z,\varepsilon) = u - \Big(R + x_2\frac{\partial L}{\partial x_1}\Big)\Big(z + i_d\Big) - \varepsilon\,\frac{di_d}{dt}$$

The input u will be a state feedback based control, it is thus a function of the state $u = u(x,z)$.

3. CONTROL DESIGN

The objective of this section is to design a control law for the voltage input u such that the closed-loop system is asymptotically stable. The singular perturbation modeling (8) enables to emphasize the two time-scale dynamics with the so-called *reduced system* (with a slow dynamic) and *boundary-layer system* (with a fast dynamic).

3.1 Reduced system and boundary-layer system

First, let us begin with the following lemma that defines the equilibrium point.

Lemma 1. If $u(0,0) = Ri_d(0)$, the origin $(x^* = 0, z^* = 0)$ is the unique equilibrium point of (8).

Proof 1. From the first condition $f(x,z) = 0$, it can be readily seen that $x_1^* = x_2^* = 0$. The third line gives

$$\begin{aligned} 0 &= -\frac{\gamma_0}{m}x_0 + \frac{1}{m}\delta(x,z) \\ 0 &= -\gamma_0 x_0 + \Gamma(x + \xi^*) - F_{mag}(r, z + i_d) \\ 0 &= \Gamma\xi^* - F_{mag}(r, z + i_d) \end{aligned}$$

This last equality is true if and only if $z^* = 0$. Furthermore, assessing the first equation with $z = 0$ implies $x_0^* = 0$ too. Setting $(x = 0, z = 0)$ in the second condition $g(x,z,\varepsilon) = 0$, we have

$$g(0,0,\varepsilon) = u(0,0) - Ri_d - \varepsilon\,\frac{di_d}{dt}\Big|_{x=0,z=0}$$

knowing that

$$\frac{di_d}{dt} = \frac{d\Big(F_{mag}^{-1}(F_u, x_1 + r)\Big)}{dt} = \frac{\partial F_{mag}^{-1}}{\partial F_u}\frac{\partial F_u}{\partial \xi}\dot{\xi} + \frac{\partial F_{mag}^{-1}}{\partial (x_1 + r)}x_2$$

Then, since at the equilibrium point $\dot{\xi} = 0$ and $x_2 = 0$, one proves that $\frac{di_d}{dt}\big|_{x=0,z=0} = 0$. Finally, if the control law at the origin $u(0,0) = Ri_d$, we get $g(0,0,\varepsilon) = 0$ for all $\varepsilon > 0$. The point $(x^* = 0, z^* = 0)$ is thus the unique equilibrium point of (8).

At this stage, let us calculate the roots of $0 = g(x,z,0)$, that is when $\varepsilon = 0$, to define the *quasi-steady-state model* and thus, the two subsystems with two time-scales. This leads us to solve

$$0 = u(x,z) - \Big(R + x_2\frac{\partial L}{\partial x_1}\Big)\Big(z + i_d\Big)$$

Choosing the control law to be linear in z :

$$u = k_1 z + k_2(x), \tag{9}$$

where k_1 and $k_2(\cdot)$ are a gain and a function to be designed, the above equation has a unique solution

$$z = h(x) = \frac{k_2(x) - \Big(R + x_2\frac{\partial L}{\partial x_1}\Big)i_d}{\Big(R + x_2\frac{\partial L}{\partial x_1}\Big) - k_1} \tag{10}$$

Consequently, the reduced system is defined by

$$\dot{x} = f(x, h(x)) = Ax + B\delta(x, h(x)) \tag{11}$$

reminding that A and B are defined in (7) and $\delta(x, h(x)) = F_{mag}(x_1 + r, i_d) - F_{mag}(x_1 + r, h(x) + i_d)$. As for the boundary layer system, it is expressed as

$$\dot{z} = g(x,z,0) \tag{12}$$

$$= \Big(k_1 - \Big(R + x_2\frac{\partial L}{\partial x_1}\Big)\Big)z + k_2(x) - \Big(R + x_2\frac{\partial L}{\partial x_1}\Big)i_d \tag{13}$$

The state x being considered as a fixed parameter in this fast dynamic. However, the equilibrium point of the above system is not zero. So let define the error variable : $y = z - h(x)$ that correspond to the distance of the state z to the quasi-steady-state trajectory. Combining (8), (9) and (10), its dynamic is written

$$\begin{aligned} \dot{y} =&\ \dot{z} - \frac{\partial h}{\partial x}\dot{x} \\ =&\ \frac{1}{\varepsilon}\Big(k_1 z + k_2(x) - \Big(R + x_2\frac{\partial L}{\partial x_1}\Big)\Big(z + i_d\Big)\Big) \\ &- \frac{di_d}{dt} - \frac{\partial h}{\partial x}\dot{x} \\ \varepsilon\,\dot{y} =&\ k_1\Big(y + h(x)\Big) + k_2(x) \\ &- \Big(R + x_2\frac{\partial L}{\partial x_1}\Big)\Big(y + h(x) + i_d\Big) - \varepsilon\frac{di_d}{dt} - \varepsilon\frac{\partial h}{\partial x}\dot{x} \\ =&\ \Big(k_1 - \Big(R + x_2\frac{\partial L}{\partial x_1}\Big)\Big)y + k_2(x) \\ &+ \Big(k_1 - \Big(R + x_2\frac{\partial L}{\partial x_1}\Big)\Big)h(x) \\ &- \Big(R + x_2\frac{\partial L}{\partial x_1}\Big)i_d - \varepsilon\Big(\frac{di_d}{dt} + \frac{\partial h}{\partial x}\dot{x}\Big) \\ =&\ \Big(k_1 - \Big(R + x_2\frac{\partial L}{\partial x_1}\Big)\Big)y - \varepsilon\Big(\frac{di_d}{dt} + \frac{\partial h}{\partial x}\dot{x}\Big) \end{aligned}$$

Considering the new time variable $\tau = t/\varepsilon$, that corresponds to the fast time scale, the new boundary layer system is given by:

$$\begin{aligned} \frac{dy}{d\tau} =&\ g(x, y + h(x), 0) \\ =&\ \Big(k_1 - \Big(R + x_2\frac{\partial L}{\partial x_1}\Big)\Big)y \end{aligned} \tag{14}$$

It is worthy to notice that this dynamic does not depend on the control term $k_2(x)$. This latter will be useful later to control the quasi-steady-state model.

3.2 Stability conditions

Firstly, one aims at proving stability of the two subsystems (11)-(14) by finding a Lyapunov function for each of them independently before designing a stability condition for the whole system. With this two-step approach, we intend to design a control law with a reduced complexity for the sake of implementation. First of all, taking into account some physical features of the system, some assumptions are stated.

Assumption 1. The state x belongs to the compact set

$$x \in D_x = \{x \in \mathbb{R}^n \mid \|x\|_2 \leq \kappa\}$$

Assumption 2. The rate of change of the magnetic force w.r.t. the current, for any airgap, is bounded

$$\frac{|F_{mag}(p,i_2)-F_{mag}(p,i_1)|}{|i_2-i_1|}=\frac{|\delta(x,i_1-i_2)|}{|i_2-i_1|}\leq\alpha_1$$

Such an upperbound can be computed based on the experimental data plotted in Figure 2.

Assumption 3. The variation of L w.r.t. the airgap has been computed from a numerical simulations campaign. With the finite element method software COMSOL and also the electrical engineering software PLECS. For the latter, a reluctance network has been designed to model the magnetic circuit and to characterize the system inductance (see Deschaux et al. (2018); Deschaux (2020)). Then, a bound on $|\frac{\partial L}{\partial x_1}|$ can be provided. From Assumption 1, the velocity $|x_2|$ is also bounded. Then an upperbound for the following expression can be estimated :

$$\left|x_2\frac{\partial L}{\partial x_1}\right|\leq\alpha_2$$

This first lemma shows the asymptotic stability of the reduced system alone and provides an expression for the term $k_2(\cdot)$ in the global control law (9).

Lemma 2. Defining the second part of the control law (9) as

$$k_2(x)=\Big(R+x_2\frac{\partial L}{\partial x_1}\Big)i_d=\Big(R+x_2\frac{\partial L}{\partial x_1}\Big)\,F_{mag}^{-1}(F_u,x_1+r) \tag{15}$$

there exists $P\in\mathbb{R}^{3\times3}$ a positive definite matrix such that the quadratic function $V(x)=x^TPx$ is a Lyapunov function for the reduced system (11).

Proof 2. Let us consider the Lyapunov candidate function $V(x)=x^TPx$. Its derivative along the trajectory of the reduced system (11) equals

$$\dot{V}(x)=x^T\Big(A^TP+PA\Big)x+2x^TPB\delta(x,h(x)) \tag{16}$$

Reminding that $h(x)$ is defined in (10), let us set the second part of the control law (9) as (15). Then, we have $h(x)=0$ and thus $\delta(x,h(x))=0$. Hence, the negative definiteness of $\dot{V}(x)$ (16) boils down to the simple condition $A^TP+PA<0$. Since A is Hurwitz by design, with a virtual state feedback (5), there always exists a matrix $P>0$ such that the condition holds.

Remark 1. It is important to note that this particular choice (15) for $k_2(x)$, which cancels $h(x)$, allows to enforce the slow dynamic of the reduced system to match the ideal prescribed mechanical dynamic (6). A simpler control law $k_2(x)=Ri_d$ could have been considered, and it can be shown that the reduced system (11) remains stable despite the perturbation term $\delta(x,h(x))$ with $h(x)$ being then equals to

$$h(x)=\frac{-\frac{\partial L}{\partial x_1}i_d}{\Big(R+x_2\frac{\partial L}{\partial x_1}\Big)-k_1}x_2$$

However, in that case, once the fast dynamic (current dynamic re-expressed as y) has converged, the quasi-steady-state trajectory will be different from the requirements specified in (6) for the expected mechanical behavior.

This second lemma provides a condition for tuning the gain k_1, from the global control law (9), to ensure the asymptotic stability of the boundary-layer system alone.

Lemma 3. Under Assumption 3, for any gain $k_1\in\mathbb{R}$ verifying the condition

$$k_1<R-\alpha_2 \tag{17}$$

then the quadratic function $W(y)=q\,y^2$, $\forall q\in\mathbb{R}_+^*$, is a Lyapunov function for the boundary-layer system (14).

Proof 3. Let us define the Lyapunov candidate function $W(y)=\frac{1}{2}q\,y^2$, with $q\in\mathbb{R}_+^*$ a positive scalar. Its derivative along the trajectory of the boundary layer system (14) equals

$$\begin{aligned}\frac{\partial W}{\partial y}g(x,y,0)&=qy^2\Big(k_1-R-x_2\frac{\partial L}{\partial x_1}\Big)\\&\leq qy^2\Big(k_1-R+\alpha_2\Big)\end{aligned}$$

The transition from the first line to the second one stems from Assumption 3. Hence, the derivative is negative definite if the condition (17) holds.

At this stage, we have exhibited a Lyapunov function for each subsystem (11) and (14), we are now in position to prove the local asymptotic stability of the whole closed loop system.

Theorem 1. Under Assumptions 1, 2, 3, there exists k_1 sufficiently large such that the closed loop system (3), (9), (15) is locally asymptotically stable.

Proof 4. The closed loop system is driven by the following equations:

$$\begin{aligned}\dot{x}&=f(x,y)\\\varepsilon\dot{y}&=g(x,y,\varepsilon)\end{aligned} \tag{18}$$

with

$$\begin{aligned}f(x,y)&=Ax+B\delta(x,y)\\g(x,y,\varepsilon)&=\left(k_1-\Big(R+x_2\frac{\partial L}{\partial x_1}\Big)\right)y-\varepsilon\frac{di_d}{dt}.\end{aligned}$$

Let us consider a Lyapunov function composed by the two Lyapunov functions defined in Lemma 2 and Lemma 3:

$$V_g(x,y)=V(x)+W(y)$$

For all $(x,y)\in\mathcal{D}_x\times\{y\in\mathbb{R}\mid\|y\|_2\leq\kappa_y\}$, where $\kappa_y>$ is any positive scalar, V_g is positive definite. The time derivative of V_g along the trajectories leads to the following expression:

$$\begin{aligned}\dot{V}_g(x,y)&=\frac{\partial V(x)}{\partial x}\dot{x}(t)+\frac{\partial W(y)}{\partial y}\dot{y}(t)\\&=x^T\Big(A^TP+PA\Big)x+2qy^2\Big(k_1-R-x_2\frac{\partial L}{\partial x_1}\Big)\\&\quad+2x^TPB\delta(x,y)-2q\varepsilon y^T\frac{di_d}{dt}\end{aligned}$$

The first two terms corresponds to the expressions obtained in proofs of lemmas when the two subsystems are studied independently. They contribute to the negativity of the Lyapunov function derivative. The last two terms stem from the interconnection between the reduced system and the boundary layer system. Let consider the term $-2q\varepsilon y^T\frac{di_d}{dt}$, which can be bounded by:

$$q\varepsilon\beta y^Ty+\frac{q\varepsilon}{\beta}\Big(\frac{\partial id}{\partial x}(Ax+B\delta(x,y))\Big)^T\Big(\frac{\partial id}{\partial x}(Ax+B\delta(x,y))\Big)$$

with $\beta>0$, an extra free positive decision variable. Furthermore, the desired current $i_d(x)$ can be evaluated through the expression of the desired force $F_u=F_{mag}(x_1+r,i_d(x))$ which is a linear function of x. As the magnetic

force applied to the mechanical system F_{mag} is a continuously differentiable function and assuming that x is bounded, there exists $\alpha_3 > 0$ such that

$$\frac{\partial id}{\partial x}^T \frac{\partial id}{\partial x} < \alpha_3^2,$$

One obtains therefore:

$$-2q\varepsilon y^T \frac{di_d}{dt} \leq q\varepsilon\beta y^T y + \frac{q\varepsilon\alpha_3^2}{\beta}(Ax + B\delta(x,y))^T(Ax + B\delta(x,y))$$

Hence, an uppperbound for V_g can be estimated as:

$$\dot{V}_g(x,y) \leq \begin{bmatrix} x \\ \delta(x,y) \\ y \end{bmatrix}^T M \begin{bmatrix} x \\ \delta(x,y) \\ y \end{bmatrix},$$

where

$$M = \begin{bmatrix} M_{11} & PB + \frac{q\varepsilon\alpha_3^2}{\beta}A^T B & 0 \\ \star & \frac{q\varepsilon\alpha_3^2}{\beta}B^T B & 0 \\ \star & \star & q\varepsilon\beta + q(k_1 - R + \alpha_2) \end{bmatrix}$$

with $M_{11} = A^T P + PA + \frac{q\varepsilon\alpha_3^2}{\beta}A^T A$. Furthermore, invoking Assumption 2, the function $\delta(x,y)$ is bounded as:

$$\delta^T(x,y)\delta(x,y) \leq \alpha_1^2 y^T y$$

Then, using the S-procedure, if there exists $\gamma > 0$ such that the

$$\begin{bmatrix} x \\ \delta(x,y) \\ y \end{bmatrix}^T M \begin{bmatrix} x \\ \delta(x,y) \\ y \end{bmatrix} - \gamma\Big(\delta^T(x,y)\delta(x,y) - \alpha_1^2 y^T y\Big) < 0$$

then $\dot{V}_g(x,y)$ is negative definite for all $(x,y) \in \mathcal{D}_x \times \{y \in \mathbb{R} \mid \|y\|_2 \leq \kappa_y\}$, and therefore the closed loop system is locally asymptotically stable. Therefore, the last sufficient stability condition is equivalent to ensure that the matrix

$$\begin{bmatrix} M_{11} & PB + \frac{q\varepsilon\alpha_3^2}{\beta}A^T B & 0 \\ \star & \frac{q\varepsilon\alpha_3^2}{\beta}B^T B - \gamma & 0 \\ \star & \star & q\varepsilon\beta + q(k_1 - R + \alpha_2) + \gamma\alpha_1^2 \end{bmatrix}$$

is negative definite.

Furthermore, for sufficiently large $\gamma > 0$, there exists P such that

$$\begin{bmatrix} A^T P + PA + \frac{q\varepsilon\alpha_3^2}{\beta}A^T A & PB + \frac{q\varepsilon\alpha_3^2}{\beta}A^T B \\ \star & \frac{q\varepsilon\alpha_3^2}{\beta}B^T B - \gamma \end{bmatrix} < 0$$

Lastly, $\forall\gamma, \epsilon, \beta, q$, there exists $k_1 > 0$ such that

$$q\varepsilon\beta + q(k_1 - R + \alpha_2) + \gamma\alpha_1^2 < 0,$$

Regrouping the last two arguments, there exists k_1 such that $\dot{V}_g$ is negative definite for all $(x,y) \in \mathcal{D}_x \times \{y \in \mathbb{R} \mid \|y\|_2 \leq \kappa_y\}$, which concludes the proof.

4. SIMULATION RESULTS

The proposed methodology is now illustrated with a numerical example. The actuator of Figure 1, described by the model (3), is simulated with parameters set as: $m = 200\ g$, $\lambda = 50\ N.s/m$, $K = 15.10^3\ N/m$ and $l_0 = 5.10^{-3}\ m$. The moving part position is initialized at $p(0) = 0.7\ mm$, that is the airgap is open because of the spring force. The initial values for the velocity v and the current i are naturally set to zero. The simulation test is to drive the position p to the setpoint $r = 0.5\ mm$. Following figures show the simulation results of the complete system (18) for different values of $k_1 = \{-200, -500, -1000, -2000\}$, along with the simulation of the reduced system (11) corresponding to the desired dynamic for the mechanical subsystem.

First, it can be observed the whole state (x,y) converges to 0, meaning that the physical state (ξ, i) converges to the desired equilibrium, especially the position p toward the setpoint r. Simulations depicted in Figures 3 and 4 show that the position and velocity trajectories get closer to the ideal mechanical dynamic as the absolute value of gain k_1 is increased (see also the phase plane in Figure 7). As expected, the more k_1 is negative the faster the boundary layer system (14) converges to 0, as shown in Figure 5, and the decoupling of the two time-scale system is valid. Note that as long as y has not converged there is in the x-system a force $\delta(x,y)$ that deviates the closed-loop mechanical subsystem dynamic from the one designed based on some specifications (see Figures 6). This force affects the acceleration of the moving part, and thus its integral influences the velocity x_2. Of course, as y is slower (for a smaller absolute value of k_1), the integral value δ is larger. All trajectories of y (and thus δ) being anyway very fast compared the x, these influences on velocity appears as a change of the initial condition. This reasoning explains the different amplitudes of the velocity x_2 around the initial time (see Figure 4).

At last, the effect of a disturbance force F_d affecting the acceleration of the moving part has been simulated. A step like disturbance of $5\,N$ was applied at time $t = 0.8\,s$. The evolution of the position is plotted in Figure 8. The integral action appended to the model in (4) enables to compensate for a non-vanishing disturbance. The gain k_1 has no effect on the response to F_d. That was expected since the disturbance appears in the mechanical subsystem and not in the electrical one, the fast dynamic where k_1 is effective.

5. CONCLUSION

In this paper, we have designed a novel control strategy for electromagnetic actuators. Compared to most papers of the literature on this topic, we have considered a more accurate model, especially taking into account the varying nature of the inductance and the magnetic saturation of the force. A augmented model has been built to embed an integral action and to ensure accuracy for the mechanical subsystem, despite some disturbances in the balance of forces. A nonlinear control has been designed based on a singular perturbation reformulation. The choice of this approach intended to design a simpler control law expression for sake of implementation, compared to backstepping

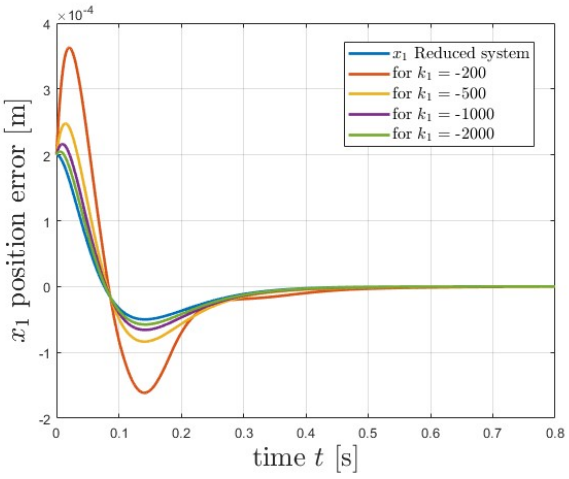

Fig. 3. *Plot of the position deviation w.r.t. the reference* $x_1 = p - r$.

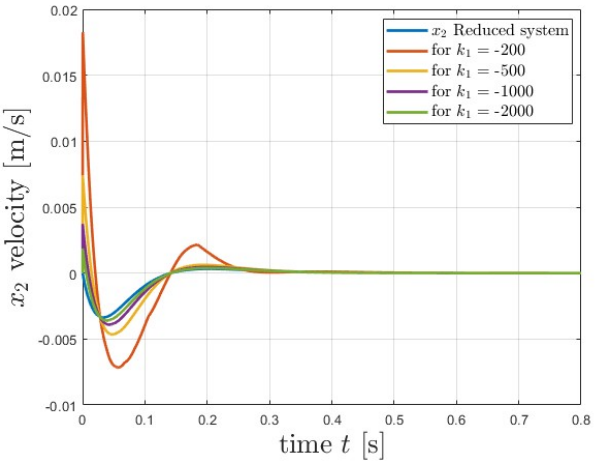

Fig. 4. *Plot of the velocity* $x_2 = v$.

and sliding mode controls, considering decoupled systems thanks to the two time scale dynamics (reduced and boundary layer systems). Simulations validate the theory and shows promising result before experimental tests.

REFERENCES

Boldea, I. (2003). Linear electromagnetic actuators and their control: A review. *EPE Journal (European Power Electronics and Drives Journal)*, 14.

Chen, M.Y., Tsai, C.F., and Fu, L.C. (2004). Design and control of a 2-dimensional electro-magnetic suspension actuator. In *Proceedings of the 2004 IEEE International Conference on Control Applications, 2004.*, volume 1, 93–98 Vol.1.

Cugat, O., Delamare, J., and Reyne, G. (2003). Magnetic micro-actuators and systems (magmas). *IEEE Transactions on Magnetics*, 39(6), 3607–3612.

Deschaux, F. (2020). *Analyse et synthèse du système de commande d'un détendeur électronique pour applications spatiales.* Ph.D. thesis, INSA, Toulouse, France. URL `http://www.theses.fr/2020ISAT0029/document`.

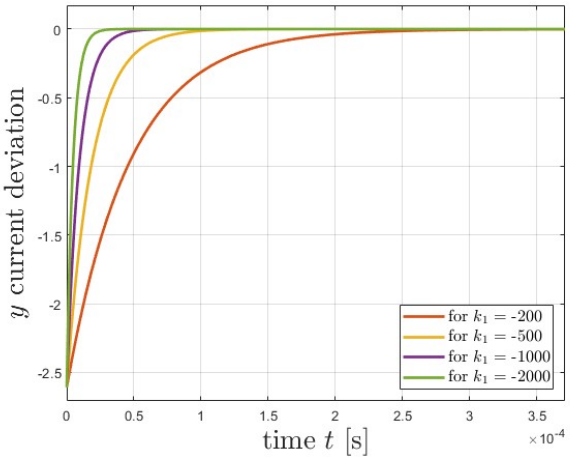

Fig. 5. *Plot of the current deviation w.r.t. the suitable current for the desired mechanical dynamic* $y = i - i_d$.

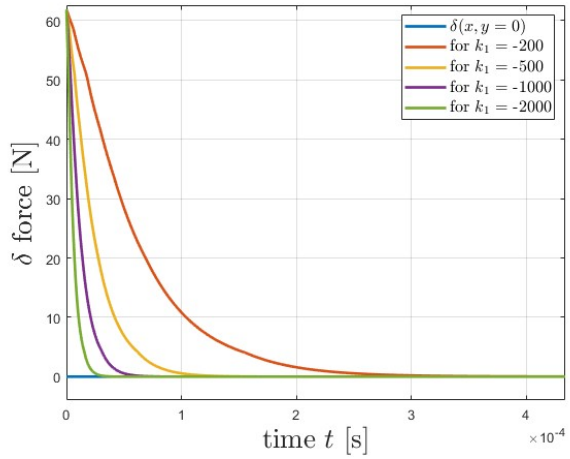

Fig. 6. *Plot of the force deviation* $\delta(x, y)$.

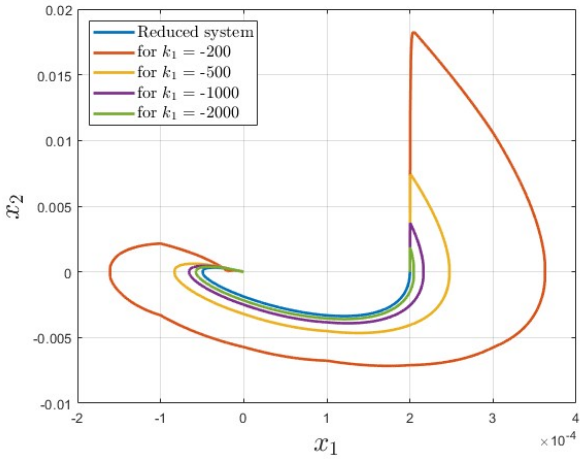

Fig. 7. *Representation of the mechanical state variables in the phase plane.*

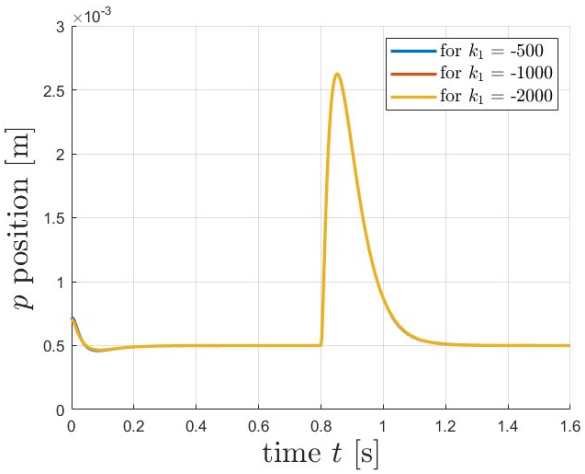

Fig. 8. *Representation of the mechanical state variables in the phase plane.*

Deschaux, F., Gouaisbaut, F., and Ariba, Y. (2018). Nonlinear control for an uncertain electromagnetic actuator. In *2018 IEEE Conference on Decision and Control (CDC)*, 2316–2321.

Deschaux, F., Gouaisbaut, F., and Ariba, Y. (2019). Magnetic force modelling and nonlinear switched control of an electromagnetic actuator. In *2019 IEEE 58th Conference on Decision and Control (CDC)*, 1416–1421.

Di Cairano, S., Bemporad, A., Kolmanovsky, I., and Hrovat, D. (2007). Model predictive control of magnetic automotive actuators. In *2007 American Control Conference*, 5082–5087.

Foo, E. and Goodall, R. (2000). Active suspension control of flexible-bodied railway vehicles using electro-hydraulic and electro-magnetic actuators. *Control Engineering Practice*, 8(5), 507–518.

Forrai, A. (2018). Modeling, system identification, and control of electromagnetic actuators. *Actuators*.

Forrai, A., Ueda, T., and Yumura, T. (2007). Electromagnetic actuator control: A linear parameter-varying (lpv) approach. *IEEE Transactions on Industrial Electronics*, 54, 1430–1441.

Jin, J., Yih, T., Higuchi, T., and Jeon, J.U. (1998). Direct electrostatic levitation and propulsion of silicon wafer. *IEEE Transactions on Industry Applications*, 34(5), 975–984.

Kahveci, N.E. and Kolmanovsky, I.V. (2010). Control design for electromagnetic actuators based on backstepping and landing reference governor. *IFAC Proceedings Volumes*, 43, 393–398.

Khalil, H.K. (2002). *Nonlinear systems; 3rd ed.* Prentice-Hall, Upper Saddle River, NJ.

Kokotović, P., Khalil, H.K., and O'Reilly, J. (1999). *Singular Perturbation Methods in Control: Analysis and Design*. Society for Industrial and Applied Mathematics.

Lee, H.W., Kim, K.C., and Lee, J. (2006). Review of maglev train technologies. *IEEE Transactions on Magnetics*, 42(7), 1917–1925.

Mercorelli, P., Lehmann, K., and Liu, S. (2003). Robust flatness based control of an electromagnetic linear actuator using adaptive pid controller. 3790–3795. IEEE.

Mercorelli, P. (2012). An antisaturating adaptive preaction and a slide surface to achieve soft landing control for electromagnetic actuators. *IEEE/ASME Transactions on Mechatronics*, 17(1), 76–85.

Mercorelli, P. (2017). A geometric approach for the design and control of an electromagnetic actuator to optimize its dynamic performance. In *2017 18th International Carpathian Control Conference (ICCC)*, 462–467. IEEE.

Nguyen, T., Leavitt, J., Jabbari, F., and Bobrow, J.E. (2007). Accurate sliding-mode control of pneumatic systems using low-cost solenoid valves. *IEEE/ASME Transactions on Mechatronics*, 12(2), 216–219.

Peterson, K., Grizzle, J., and Stefanopoulou, A. (2006). Nonlinear control for magnetic levitation of automotive engine vales. *IEEE Transactions on Control Systems Technology*, 14(2), 346–354.

Robert Koch, C., Lynch, A.F., and Chladny, R.R. (2002). Modeling and control of solenoid valves for internal combustion engines. *IFAC Proceedings Volumes*, 35(2), 197–202. 2nd IFAC Conference on Mechatronic Systems, Berkeley, CA, USA, 9-11 December.

Schwarzgruber, T., Trogmann, H., Passenbrunner, T.E., Fizek, S., and Dolovai, P. (2012). Nonlinear control of an electro-magnetic actuator under highly dynamic disturbances. In *2012 IEEE International Conference on Control Applications*, 974–979.

Zhang, X., Lai, L., Zhang, L., and Zhu, L. (2022). Hysteresis and magnetic flux leakage of long stroke micro/nanopositioning electromagnetic actuator based on maxwell normal stress. *Precision Engineering*, 75, 1–11.